Wide-Band Photonically Phased Array Antenna Using Vector Sum Phase Shifting Approach

Lam Anh Bui, *Member, IEEE*, Arnan Mitchell, *Member, IEEE*, Kamran Ghorbani, Tan-Huat Chio, Sana Mansoori, and Elias R. Lopez, *Student Member, IEEE*

***Abstract*—In this paper, a wide-band photonically phased array antenna is demonstrated. The array configuration consists of a 4 $\times$ 1 Vivaldi single-polarization antenna array and an independent photonic phasing system for each element. The phasing network of this array is implemented using two novel photonic phase shifters based on the vector summation approach. A vector sum phase shifter (VSPS), which exhibits a frequency-linear characteristic from dc to 15 GHz and can be continuously tuned from 0 to 100°, is presented. A second-order VSPS (SO-VSPS), a modification of the VSPS that is capable of 0–430° phasing range, is also demonstrated. This paper presents the operation and characterization of each component of the array, including the radiating elements and the various photonic phase shifters and, finally, a demonstration of the combined system. A discussion on the practicality of this system for airborne applications is presented, along with suggestions for simplification and improvement.**

***Index Terms*—Microwave photonics and phase shifter, phased array antenna, true time delay.**

I. Introduction

PHASED array antennas (PAAs) have attracted a great deal of research interest due to their capability to provide much flexibility that is difficult to achieve with non array antenna systems. A PAA comprises two major components: the antenna array and the beam forming network (BFN). The antenna array consists of a number of distributed radiating elements often arranged in a regular one- or two-dimensional grid. The BFN usually provides individual control of phase and magnitude for each of the array elements. Electronic beam scanning of the PAA is achieved by varying the phase of the excitation of the elements. For narrow-band applications, the phase of the elements can be controlled using phase shifting techniques [1]. For some applications (pulsed radar, for example [2]), a relatively broad instantaneous bandwidth is required, and thus broadband phase shifting or time shifting techniques must be used [3].

Photonics is an attractive technology for PAA due to its broad bandwidth, immunity to electromagnetic interference, light weight, and flexible system implementation [4]. Many investigations over the past years have attempted to realize photonic PAA capable of broadband beamforming [5]–[8]. A drawback of these photonic systems is the high component and installation cost.

A previous investigation has proposed and demonstrated a photonically realized RF phase shifter for compactness. This device was called the vector sum phase shifter (VSPS) [9]. This paper presents the VSPS performance in a practical phased array antenna system. It is thus demonstrated the VSPS as a broadband, true time delay (TTD) like solution that could be economically and practically realized for PAA applications.

Although the VSPS exhibits excellent phase linearity, the device phasing range is limited to 100°. It is possible to exploit the VSPS cyclic frequency behavior and utilize the higher order response of the VSPS to obtain a larger phasing range at the expense of reduced bandwidth. A device operating on this principle was demonstrated using second-order response of the VSPS, and was thus called the second-order vector sum phase shifter (SO-VSPS) [10].

Using the VSPS and the SO-VSPS as phase shifting devices, a preliminary demonstration of a three-element PAA has been presented with beam scanning up to 30° [11]. This demonstration has shown the potential of the proposed photonic phasing technique. It was found that the suboptimal beam forming quality of the demonstrated system was attributed to polarization instability throughout the system. In this investigation, we reimplement the system in [11] and demonstrate a full four element PAA with good beam stability.

This paper is arranged as follows. Section II presents an overview of the PAA system indicating each of the subcomponents. The radiating element is presented in Section III, along with radiation patterns of the phased array using mechanical phase shifters. The first photonic phase shifter implementation (the VSPS) is introduced in Section IV. The phase and amplitude responses of the system are presented, demonstrating continuously variable phase shifting of 0–100°, scaling almost linearly from dc–15 GHz. The second photonic phase shifter implementation, the SO-VSPS, is introduced in Section V. A demonstration of how the second order of the VSPS response can be used with a frequency invariant phase shifter (FIPS) to provide continuous phase shifting in the range 0–430° from 8 to 16 GHz is presented. Section VI presents the integration of various phase shifters to form the photonic BFN. The performance of the photonically PAA is presented in Section VII. A discussion on system practicality and proposed improvements are presented in Section VIII. The concluding remarks are given in Section IX.

Manuscript received February 22, 2005; revised May 29, 2005. This work was supported by DSO National Laboratories, the Australian Photonics Cooperative Research Centre, and RMIT University.

L. A. Bui, A. Mitchell, K. Ghorbani, S. Mansoori, and E. R. Lopez are with the School of Electrical and Computer Engineering, RMIT University, Melbourne 3001, Australia (e-mail: l.bui@ieee.org).

T.-H. Chio is with DSO National Laboratories, Singapore 118230, Singapore (e-mail: ctanhuat@dso.org.sg).

Digital Object Identifier 10.1109/TAP.2005.858868

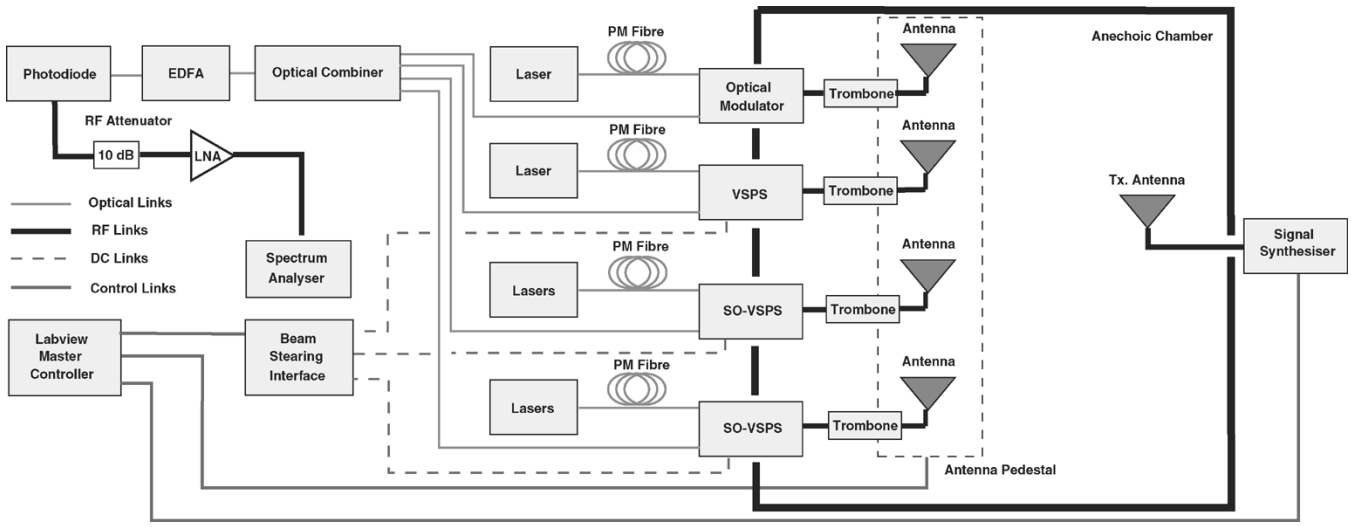

Fig. 1. Schematic diagram and the experimental setup of the photonically PAA. Distinct optical wavelengths are utilized for the phase shifters.

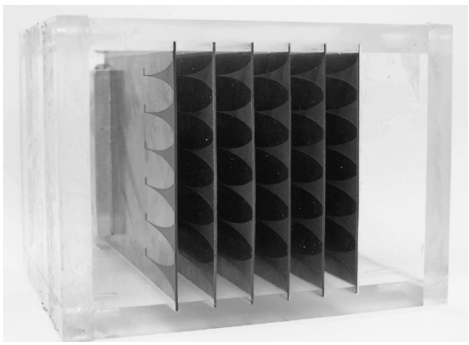

Fig. 2. Vivaldi antenna array.

II. Photonically PAA System

A schematic diagram of the photonically PAA system is presented in Fig. 1. The array consists of a radiation module fed by four independent phase shifting elements. Three distinct phase shifters have been implemented, including a simple RF photonic link, VSPS, and SO-VSPS. The four phase shifting elements are combined and amplified optically and detected with a single photodetector. It is worth noting that only the modulators in each system must be located at the antenna, with all other components being remoted using optic fiber.

III. Radiating Element and Antenna Array

The array antenna [12], [13] was designed and fabricated by DSO National Laboratories, Singapore, and was made available for this investigation. It consists of six subarrays uniformly spaced 12 mm apart as shown in Fig. 2. Within each subarray, there are four radiating elements and two dummy elements. The four central elements are combined in phase through a network of Wilkinson combiners and the remaining two elements are terminated in 50 Ω.

It is anticipated that a finite number of array elements would present an abrupt truncation of the array, which manifests itself as the distortion of the subarray patterns. To reduce this distortion, the two outside subarrays are terminated in 50 Ω. This effectively creates a 1×4 linear array surrounded by a ring of dummy elements terminated in a 50 Ω load.

Initially, the antenna array was characterized by measuring the return loss and the radiation pattern of an individual subarray. This was performed by measuring one subarray with the other subarrays terminated in 50 Ω. It was found that the central four subarrays exhibited similar pattern and better than 10 dB return loss between 10 and 14 GHz. Below 10 GHz, a significant coupling between elements causing variation of radiation pattern from subarray to subarray was observed. Above 16 GHz, the high test range loss and the appearance of grating lobes for the array beam scanned to 30° were anticipated. The PAA was thus analyzed within the band from 10 to 14 GHz.

Having measured each individual subarray, the antenna array was then characterized for beam scanning performance. A BFN was constructed using mechanical phase shifters and was used in place of the photonic phasing network of Fig. 1. The phase shifters used for this experiment were mechanically variable trombone microwave lines. They have a specified bandwidth of dc to 18 GHz, an insertion loss less than 1.5 dB, and a maximum phase tuning range just over 400° at 18 GHz.

To simplify the experiment, beam scanning is limited to one direction. The first phase shifter was therefore maintained at zero phase setting for all beam angles. Taking the response of the first phase shifter as a reference, the response of other phase shifters was set with the help of a network analyzer (NA). The PAA was measured inside an anechoic chamber. Fig. 3 presents the measured radiation patterns of the mechanically PAA.

Assuming an ideal TTD phase shifting characteristic, the array factor was calculated for each beam angle and multiplied by the measured radiation pattern of a single subarray. The theoretical pattern was predicted as this product. The prediction is presented in broken lines together with the measured patterns in Fig. 3.

It is evident from Fig. 3 that there is a good agreement between measurements and predictions. This verifies that the PAA behave in accordance with simple array factor theory. It is also

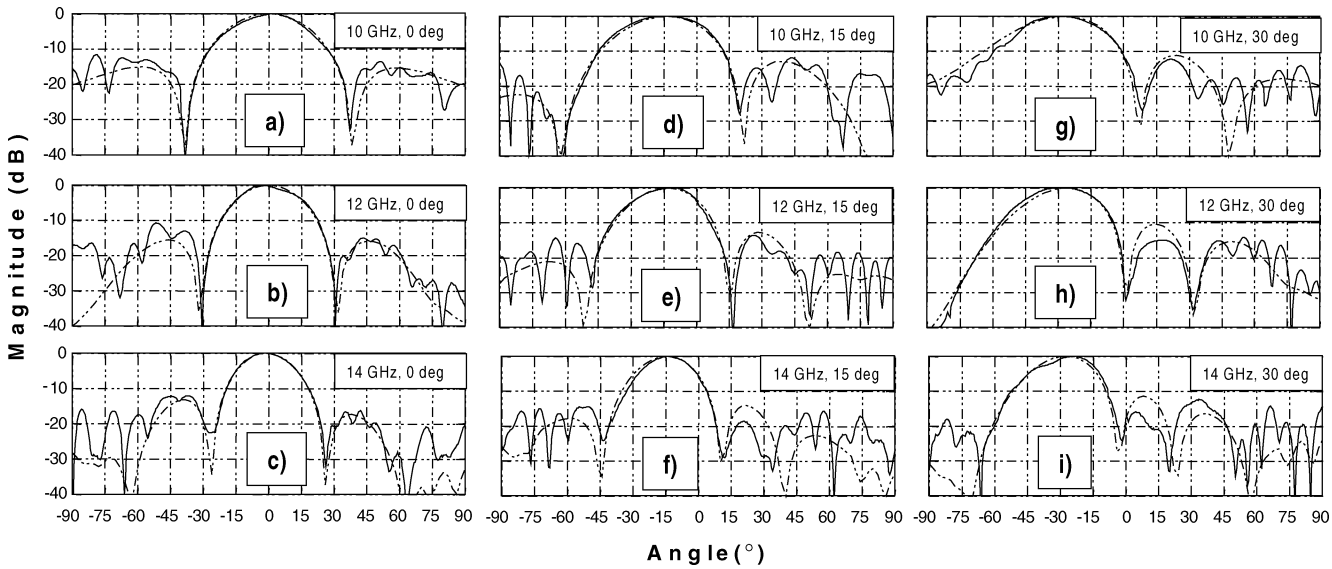

Fig. 3. H-plane patterns of the PAA using mechanical phase shifters with beam scanned to (a)–(c) 0°, (d)–(f) 15°, and (g)–(i) 30°. Measured and computed patterns are presented in solid and broken lines, respectively. All patterns are normalized to have maximum values of 0 dB for ease of comparison.

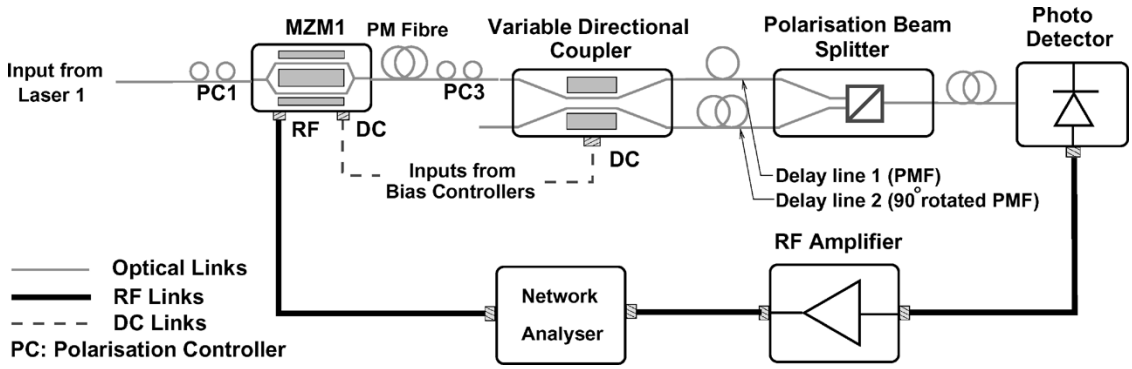

Fig. 4. VSPS schematic and experimental setup.

anticipated that the beam patterns of Fig. 3 will be useful as a benchmark for comparison with the photonic phasing system that is to be presented.

IV. The Vector Sum Phase Shifter

A. Principle of Operation

A detailed description of the VSPS is presented elsewhere [9], [14]. A brief explanation of the VSPS is given here for the reader's convenience. The architecture of the VSPS is presented in Fig. 4. The radio-frequency (RF) signal to be phase shifted is modulated onto an optical carrier using an external Mach–Zehnder modulator (MZM). The modulated carrier is split into the ratio $x : 1 - x$ by a variable optical directional coupler (VDC). Since the RF signal is an intensity modulation on the optical carrier, the amplitude of this signal is split by the same ratio. The split signals are then transmitted through optical delay lines of different lengths. The two differentially delayed signals are then summed using an optical combiner and detected using a photodetector. By varying the component relative amplitudes (by adjusting the splitting ratio of the VDC), a continuous variation of phase shifts is obtained.

B. Single Element Performance

For a maximum beam angle of 30°, the second element of the photonic BFN required a phase shift of 86.4° at 12 GHz. The VSPS was utilized for this element. The resonant frequency of the VSPS can be calculated from this phasing requirement as $(12 \times 180^\circ)/86.4^\circ = 25$ (GHz). The optical path length difference can be directly derived from the resonant frequency and is equal to $\Delta L = 4\,\mathrm{mm}$.

The VSPS is implemented as outlined in Fig. 4. Orthogonal polarizations are utilized in the two delay paths to avoid coherent beating when combining the optical carriers. The VSPS was measured before it was integrated into the photonic BFN to ensure that the desired phasing characteristics were available. Fig. 4 presents the experimental setup to analyze the VSPS. Configuring the phase shifter to a given phase shift was achieved through nomination of a fit point. A fit point of 12 GHz was nominated, and the required phase shifts at 12 GHz were calculated for each beam angles of 0°, 15°, and 30°. Using an NA to measure the phase response of the VSPS, the VDC bias voltage was slowly adjusted until the phase response passed through the fit point. Fig. 5 presents the measured responses of the VSPS for settings of each beam angle.

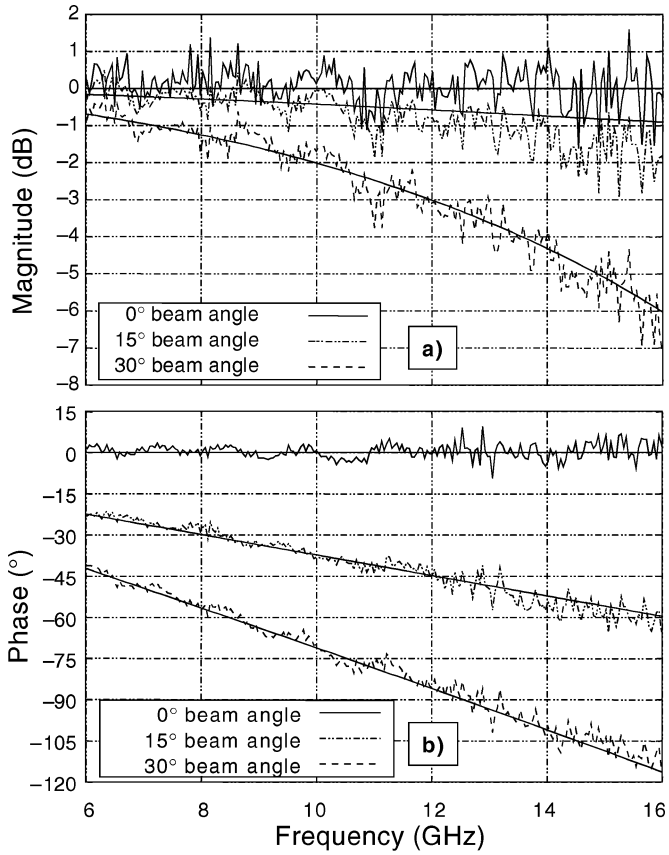

Fig. 5. Measured responses of element 2 of the photonic BFN for beam angles of 0°, 15°, and 30° respectively. Predictions are presented as thin solid lines.

To analyze the VSPS response, theoretical responses of the VSPS were computed from the device transfer function assuming ideal components and the resonant frequency of 25 GHz. These theoretical responses are presented as thin solid lines in Fig. 5. It is evident that the VSPS behaved as predicted. Toward the device resonant frequency, strong signal cancellation and phase nonlinearity limit the device bandwidth and phasing range to dc–15 GHz and 100° respectively. Within the dc–15 GHz band, the device characteristic approximates TTD.

Visible ripple is also observed in the measured responses. It is proposed that this ripple was caused by the Fabry–Perot cavity formed by signal reflections from the two end facets within the in-house fabricated VDC. Preparing the end facets of the VDC with antireflection coatings or with angle polishing would significantly reduce this reflection and hence the ripple. Although exhibiting undesirable ripple, the phase response is linear and is deemed acceptable for the demonstration purpose.

V. The Second-Order Vector Sum Phase Shifter

A. Phase Shifter Architecture

The phasing requirement for the third and fourth elements of the photonic BFN is summarized in Table I. It is evident that a phasing range of over 100° is required for both elements 3 and 4. The VSPS thus could not be used for the last two elements of the photonic BFN. It has been proposed that increasing of the VSPS phasing range can be achieved through exploiting the device second order response. A detailed explanation of this technique is available in [10]. A brief discussion of the SO-VSPS is provided below for completeness.

TABLE I
Phasing Requirements of the Photonic BFN Computed at 12 and 13.7 GHz for Scanning Angles of 0°, 15°, and 30°

Scanning Angle (°)	Element 3 Phase(°)		Element 4 Phase(°)	
	at 12 GHz	at 13.7 GHz	at 12 GHz	at 13.7 GHz
0	0	0	0	0
15	89.4	102.2	134.2	153.3
30	172.8	197.4	259.2	296.1

A schematic diagram of the SO-VSPS is presented in Fig. 6. The system incorporates a VSPS, but with a larger length difference (16.7 mm) than the VSPS presented in Section IV, creating a resonance below the desired frequency of operation. Fig. 7(a) and (b) presents the measured response of the VSPS alone. It is evident that a broad range of linear phase shifts with relatively flat amplitude response are available centered at 12 GHz in the second order of the response. To utilize this higher order response, a FIPS must be employed to raise the frequency linear phase response such that it appears to approximate TTD characteristic (monotonically approach zero). For this implementation, a FIPS consisting of two modulators fed using a 90° RF hybrid [15] is utilized.

B. Single Element Performance

The SO-VSPS consists of an FIPS cascaded with a VSPS. It is worth noting that the phase response of the VSPS at frequency of twice the device resonant frequency is always zero. The system phase response at this frequency is thus solely contributed by the FIPS [10]. It was proposed that to configure the SO-VSPS system response, two fit points should be used. One fit point is chosen at twice the resonant frequency (12 GHz) and the other fit point is arbitrarily selected (13.7 GHz). Similar to Section IV-B, the phase requirements at each fit point were calculated for each beam angle. This requirement is summarized in Table I.

Using Table I as a guideline, the FIPS was adjusted to provide the required phase offset at 12 GHz; then the VSPS was tuned to provide the required phase slope (passing through the required phase at 13.7 GHz). The measured responses of elements 3 and 4 of the photonic BFN in accordance with the phase settings of Table I are presented in Fig. 7(c)–(f) respectively. To analyze the measured responses, the theoretical responses were calculated for each phase setting of Table I assuming an ideal FIPS. The theoretical results are plotted as thin solid lines together with the measured results for easy comparison.

It is evident that the SO-VSPS can meet the phase requirements of Table I. The phase response is linear between 8–16 GHz and can be made to project monotonically to zero. Within the 8–16 GHz band, the SO-VSPS characteristic thus approximates TTD. Apart from the apparent ripple due to the VDCs and the trombone lines, the measured responses traced favorably against the theoretical predictions.

VI. The Photonic Beam Forming Network

Having demonstrated the individual phase shifters, the photonic BFN was then constructed as depicted in Fig. 1. Distinct

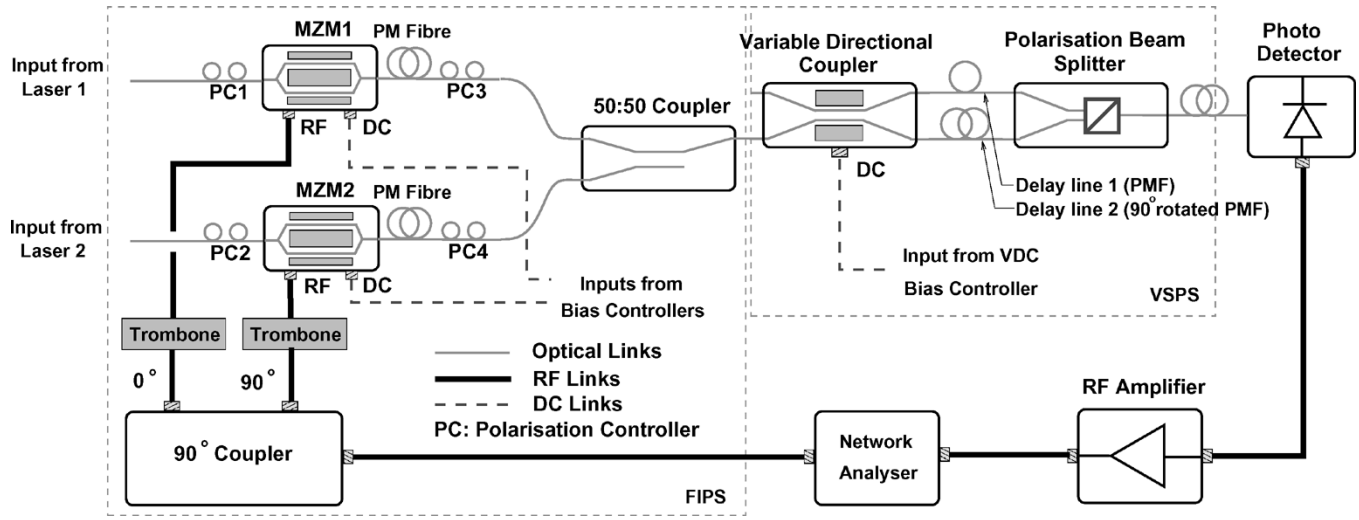

Fig. 6. SO-VSPS schematic and experimental setup. Different wavelengths are used for Lasers 1 and 2.

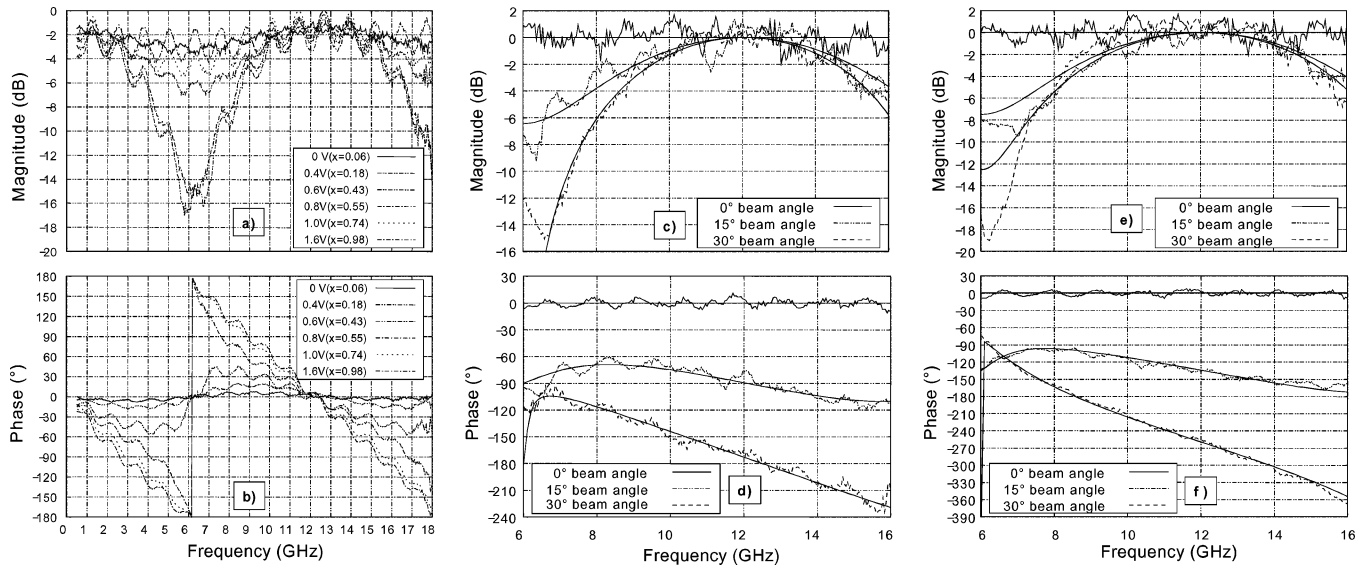

Fig. 7. Measured responses of the VSPS of (a), (b) Fig. 6, (c), (d) element 3, and (e), (f) element 4 of the photonic BFN. Various curves in (a) and (b) correspond to several settings of the VDC bias voltage (V). The x value associated with each voltage is given in parentheses. Curves of (c)–(f) correspond to photonic BFN settings for beam angles of 0°, 15°, and 30° respectively. Predicted responses are presented as thin solid lines.

lasers were utilized to provide the optical carriers for the photonic phase shifters to avoid coherent interference when these carriers were combined [16]. To compensate for various optical losses within the photonic network, the optical signal is amplified with an erbium doped fiber amplifier (EDFA) before being detected using a broadband photodetector. The output RF signal was then further amplified with a low-noise amplifier (LNA). To match the high output impedance of the photodetector with 50 Ω input impedance of the LNA, a transimpedance amplifier should be used. Such an amplifier was not available at the time of this investigation. A 10 dB RF attenuator was therefore used to dampen signal reflections due to this impedance mismatch at the expense of increased system noise figure.

A. Matching the Electrical Lengths of the Elements

Initially, when the phase shifters were integrated with the optical combiner, the electrical lengths of various elements could be different by several meters. Matching the electrical lengths was therefore necessary. This was performed in two steps. First, the time delays within each arm of the photonic BFN were measured by sending a short duration electrical pulse through the system and determining the propagation time delay with a fast oscilloscope. Knowing the time delays within each arm, fiber-optic cables were carefully cut to compensate for the propagation time difference. Using this technique, various arms of the photonic BFN were matched to within 4 cm in length (limited by the time resolution of the oscilloscope). In the second step, an NA was used to measure the phase responses of each arm after the first length compensation step. Precise fiber cleaving [17] was then performed to reduce the length difference to within ±0.5 mm. The remaining electrical lengths were finally compensated for using microwave trombone lines.

B. Matching the Amplitude Responses of the Elements

Having equalized the electrical lengths, the link gain of various arms of the photonic BFN was measured and the laser power was calibrated to ensure power balance across the array. Setting all the lasers to 1 mW output power, the link gain of

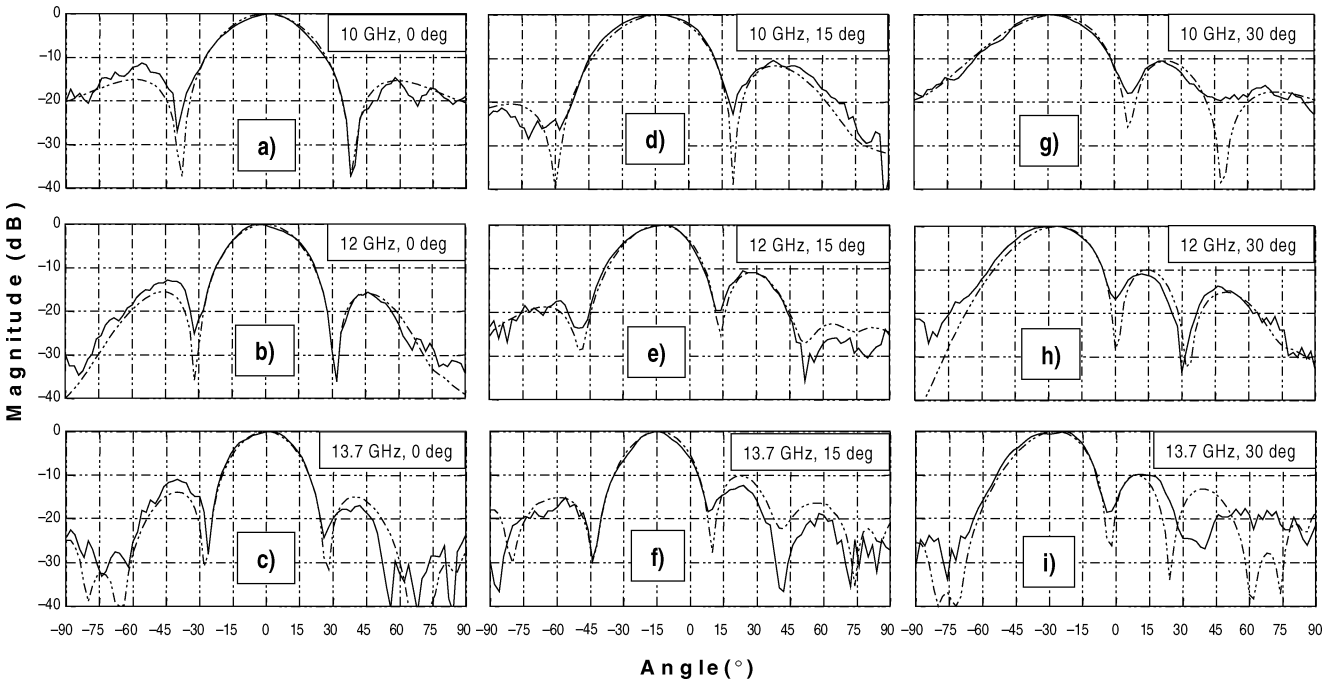

Fig. 8. H-plane patterns of the photonically PAA with beam scanned to (a)–(c) 0°, (d)–(f) 15°, and (g)–(i) 30°. Measured and computed patterns are presented in solid and broken lines, respectively. All patterns are normalized to have maximum values of 0 dB for ease of comparison.

elements 1–4 was measured. It was observed that the link responses were similar in that they exhibited a sharp gain drop at 14 GHz. This undesired behavior was attributed to the photodetector. It was suggested that measurements should not be taken at 14 GHz. Additionally, it was found that the measured gains were varied from element to element due to different insertion loss exhibited by these elements. To calibrate the BFN, the optical power of same elements was reduced so that they all exhibited the same link gain as that of the lowest gain element.

C. Discussion of the Photonic Beam Forming Network

It was anticipated that after matching the electrical lengths and calibrating the laser powers, each element of the photonic BFN exhibited identical response at zero phase setting. Taking the zero phase setting as a reference, the phase characteristics of element 2 would be similar to those of Fig. 5 and those of elements 3–4 similar to those of Fig. 7(c)–(f) respectively. It is thus evident that the phasing characteristics required for beam angles of up to 30° are indeed available.

VII. Photonically Phased Array Performance

Prior to pattern measurements in an anechoic chamber, each phase shifter of the photonic BFN was set to provide the required phase shift for a desired beam angle. This was performed as discussed in Sections IV and V for the VSPS and the SO-VSPS, respectively. For each beam angle, the array pattern measurements were taken at frequencies of 10, 12, and 13.7 GHz (rather than 14 GHz for the reason stated in Section VI-B). Fig. 8 presents the measured patterns for beam angles of 0°, 15°, and 30°, respectively.

The theoretical patterns of the photonically PAA were also computed using the array factor theory, taking into account the theoretical characteristics of the photonic phase shifters. These theoretical patterns are presented as broken lines together with the measurements in Fig. 8.

Good agreement between the predictions and measurements is evident. All patterns scan to the desired beam angles and exhibit minimal squint. This result demonstrates the TTD-like characteristics of the photonic BFN from 10 to 14 GHz. In comparison with the TTD PAA patterns of Fig. 3, the photonically PAA exhibits a slightly higher sidelobe level, although the level remains below −10 dB. The increase in sidelobe level is attributed to the amplitude variations of the VSPS and the SO-VSPS with frequency. It is suggested that techniques to reduce the amplitude imbalance of the VSPS should be investigated to improve the phase shifter and the photonic BFN bandwidth [18].

VIII. Discussion

Though the PAA was successfully demonstrated, a number of observations warrant further discussion. In particular, the stability of the phasing system and the practical requirements for implementation are discussed below.

A. System Stability

Several sources of instability have been identified through the experimental investigation of the photonically PAA. The shallow nulls evident in Fig. 8 could be attributed to instability of the relative optical power delivered to each phase shifting element. A major source of this instability was the polarization drift. It was found that the polarization drift at the input of the VSPS had the most pronounced impact on the photonic BFN response. For a polarization change from TM to TE, the optical loss through the VSPS could vary by as much as 20 dB. This was attributed to the polarization-dependent loss characteristics of

the constituent components of the phasing elements. It is therefore essential that the polarization of the optical carrier input to the VSPSs be properly aligned and maintained. This was achieved by using polarization maintaining fibers where possible. Implementing the system using polarization maintaining components would significantly improve the system stability. Alternatively, monolithic integration of the VSPS and the FIPS could also help to reduce the impact of polarization drift.

Instabilities in the photonic BFN could also be attributed to bias drift of the MZMs and the VDCs. This drift, although slow, had a pronounced effect on the FIPS performance. It is anticipated that employing bias control electronics would significantly reduce the drift and further stabilize the system.

Amplifying multiple wavelengths simultaneously could result in gain instability among different wavelength components [19], [20]. To avoid this problem, a third-generation EDFA could be used. EDFAs of this generation have built-in electronics that allow distribution of available gain among all components and sophisticated gain control strategies [21].

The system was relatively stable although no temperature control was employed. It is suggested that monitoring and feedback control electronics should be employed for the photonic BFN so that any drift could be detected and compensated accordingly. With electronic control, it should be possible to implement a simple algorithm to control the beam former electronically, hence allowing simple and fast beam scanning.

B. Practicality of Implementation

When implementing the photonic BFN, it was found that the most challenging and time-consuming task was the production of the fiber-optic cables of various lengths required for the photonic BFN. Although the fiber cables have been made with great care, it is inevitable that these fibers exhibit a variety of optical losses. The differences in the fiber loss cause variations in the VSPS device responses and give rise to response imbalance among the elements. Since this imbalance is difficult to compensate for, it is proposed that using the high birefringent (HiBi) VSPS [14] could alleviate the fiber cutting requirement and hence allow better matching of the VSPS responses between elements. However, to realize this solution, it is necessary to obtain an electronic means of polarization rotation. Investigation of this VSPS implementation is proposed for future work.

In comparison with other photonic true time delay technologies, the vector sum approach is generally simpler and less expensive. In particular, the VSPS is smaller than the Rotman lens [22], has faster response time than the fiber prism [23], and has better environmental stability than the true time delay using fiber Bragg gratings [24]. However, the VSPS is not true time delay in the sense that its characteristic only approximates TTD within a defined frequency range. The device usable bandwidth is therefore limited. The major advantage of the vector sum approach is therefore the ability to integrate the complete system into a compact unit using integrated optics.

Unlike other TTD solutions in which increasing time delay is achieved through scaling the system size, extending the VSPS phase shift is less straightforward. Several approaches have been conceived. They include 1) use of higher (third, fourth, etc.) order responses of the VSPS or 2) cascading the VSPS with compatible switched delay lines or 3) employing transversal phase shifters [18], [25]. An elegant and compact solution using polarization diversity and dispersion properties of a HiBi fiber in which distinct optical wavelengths could be employed for a single VSPS device has been proposed [14]. Investigations are currently underway to utilize these technologies to extend the phasing range and to integrate many phase shifters into a single system such that larger one- or two-dimensional phased arrays can be practically realized.

IX. Conclusion

A wide-band photonically phased array antenna has been demonstrated. A Vivaldi array antenna has been designed and implemented and beam forming has been demonstrated using mechanical phase shifters. It was found that the phased array performed in accordance with simple array factor theory. Two photonic phase shifters have been proposed, demonstrated, and used to form the photonic beam forming network. Beam steering has been demonstrated with minor degradation in sidelobe performance in comparison with the true time delay performance. This degradation was attributed to the amplitude degradation due to the resonant nature of the photonic phase shifters. It is proposed that techniques to reduce the phase shifter amplitude degradation would improve the phase shifter bandwidth, and hence improve the phased array performance. An initial investigation can be found in [18].

The realization of the VSPS and SO-VSPS phase shifters for the photonic BFN has identified some practical limitations. The most significant issue is the requirement for polarization control throughout the system. Use of polarization maintaining components would greatly simplify the demonstration.

Several improvements to the implementation and control of the system have been conceived and are currently under investigation. The requirement for fiber adapters, splices, and hybrid components throughout the phased array system has lead to increased insertion loss. Condensing the system as much as possible would reduce these losses and also the system complexity. Pursuing this idea, it may be possible to design and fabricate a device that incorporates dual MZMs and VDC components on a single $LiNbO_3$ chip. This would provide the FIPS and much of the VSPS functionality on a single chip, alleviating polarization control and loss issues.

Further, it may be possible to use wavelength-division multiplexing (WDM) techniques such that only a single device is required for all four elements. Combination of optical carriers through a WDM combiner would also incur less loss than standard 3 dB couplers.

Acknowledgment

The authors would particularly like to thank Altamar Networks Australia and the Optical Fiber Technology Centre for the loan of essential equipment, and Y. Cao and D. Welsh for their invaluable assistance.

References

[1] R. Tang and R. W. Burns, "Array technology," *Proc. IEEE*, vol. 80, pp. 173–182, Jan. 1992.

[2] P. Bradsell, "Phased arrays in radar," *Electron. Commun. Eng. J.*, pp. 45–51, Apr. 1990.
[3] J. Frank, "Bandwidth criteria for phased array antennas," in *Proc. Phased Array Antenna Symp.*, Brooklyn, NY, Jun. 1970, pp. 243–253.
[4] P. J. Matthews, "Practical photonic beamforming," in *Proc. IEEE Int. Topical Meeting Microwave Photonics*, Nov. 1999, pp. 271–274.
[5] A. N. Riza and J. B. Thompson, *Selected Papers on Photonic Control Systems for Phased Array Antennas*. Bellingham, WA: SPIE, 1997.
[6] A. P. Goutzoulis, D. K. Davies, and J. M. Zomp, "Hybrid electronic fiber optic wavelength-multiplexed system for true time-delay steering of phased array antennas," *Opt. Eng.*, vol. 31, pp. 2312–2322, Nov. 1992.
[7] H. Zmuda and E. N. Toughlian, *Photonic Aspects of Modern Radar*. Norwood, MA: Artech House, 1994.
[8] J. J. Lee, R. Y. Loo, S. Livingston, V. I. Jones, J. B. Lewis, H.-W. Yen, G. L. Tangonan, and M. Wechsberg, "Photonic wideband array antennas," *IEEE Trans. Antennas Propag.*, vol. 43, pp. 966–982, Sep. 1995.
[9] L. A. Bui, A. Mitchell, K. Ghorbani, and T. H. Chio, "Wideband RF photonic vector sum phase shifter," *Electron. Lett.*, vol. 39, pp. 536–537, Mar. 2003.
[10] ——, "Wideband RF photonic second order vector sum phase shifter," *IEEE Microw. Comp. Lett.*, vol. 15, pp. 309–311, May 2005.
[11] A. Mitchell, L. A. Bui, K. Ghorbani, S. Mansoori, W. Rowe, E. Lopez, and T. H. Chio, "Demonstration of a wideband photonic phased array using integrated optical RF phase shifter based on the vector sum approach," in *Proc. IEEE Int. Symp. Phased Array Systems Technology*, Boston, MA, Oct. 2003, pp. 199–204.
[12] T. H. Chio and D. H. Schaubert, "Parameter study and design of wideband widescan dual-polarized tapered slot antenna arrays," *IEEE Trans. Antennas Propag.*, vol. 48, pp. 879–886, Jun. 2000.
[13] H. Holter, T.-H. Chio, and D. Schaubert, "Elimination of impedance anomalies in single- and dual-polarized endfire tapered slot phased arrays," *IEEE Trans. Antennas Propag.*, vol. 48, pp. 122–124, Jan. 2000.
[14] L. A. Bui, A. Mitchell, and T. H. Chio, "Wideband vector sum phase shifter with minimal coherent interference," in *Proc. COIN Conf. Incorporating ACOFT*, Melbourne, Australia, Jul. 2003, pp. 645–648.
[15] S. T. Winnall, A. C. Lindsay, and G. A. Knight, "A wide-band microwave photonic phase and frequency shifter," *IEEE Trans. Microwave Theory Tech.*, vol. 45, pp. 1003–1006, Jun. 1997.
[16] A. Arie and M. Tur, "Phase-induced intensity noise in optical interferometers excited by semiconductor lasers with non-Lorentzian lineshapes," *J. Lightw. Technol.*, vol. 8, pp. 1–6, Jan. 1990.
[17] L. A. Bui, "Broadband photonically phased array antenna using vector sum phase shifting approach," Ph.D. dissertation, Royal Melbourne Inst. of Technology, Australia, 2004.
[18] L. A. Bui, A. Mitchell, and T. H. Chio, "Demonstration of a wideband RF photonic transversal phase shifter," presented at the *Optical Fiber Communication Conf.*, Los Angles, CA, Feb. 2004, paper FE6.
[19] T. Aizawa, T. Sakai, A. Wada, and R. Yamauchi, "Effect of spectral-hole burning on multi-channel EDFA gain profile," in *Proc. Optical Fiber Communication Conf.*, vol. 2, 1999, pp. 102–104.
[20] M. F. Krol, Y. Liu, J. J. Watkins, and M. J. Dailey, "Gain variations in optically gain clamped Erbium doped fiber amplifiers," in *Proc. Eur. Conf. Optical Communication*, vol. 1, 1998, pp. 43–44.
[21] A. Bianciotto, A. Carena, V. Ferrero, and R. Gaudino, "EDFA gain transients: Experimental demonstration of a low cost electronic control," *IEEE Photon. Technol. Lett.*, vol. 15, pp. 1351–1353, Oct. 2003.
[22] R. A. Sparks and N. Slawsby, "Eight beam prototype fiber optic Rotman lens," in *Proc. Int. Topical Meeting Microwave Photonics*, vol. 1, 1999, pp. 283–286.
[23] R. D. Esman, M. M. Frankel, J. L. Dexter, L. Goldberg, M. G. Parent, D. Stilwell, and D. G. Cooper, "Fiber-optic prism true time delay antenna feed," *IEEE Photon. Technol. Lett.*, vol. 5, pp. 1347–1349, Nov. 1993.
[24] J. L. Corral, J. Marti, S. Regidor, J. M. Fuster, R. Laming, and M. J. Cole, "Continuously variable true time-delay optical feeder for phased-array antenna employing chirped fiber gratings," *IEEE Trans. Microwave Theory Tech.*, vol. 45, pp. 1531–1536, Aug. 1997.
[25] L. A. Bui, A. Mitchell, W. G. Slade, and T. H. Chio, "Wideband variable transversal phase shifter," in *Proc. Int. Microwave Symp.*, vol. 2, Philadelphia, PA, Jun. 2003, pp. 1291–1294.

Lam Anh Bui (S'00–M'04) received the B.E. degree (with honors) in communication engineering and the Ph.D. degree from RMIT University, Melbourne, Australia, in 1997 and 2004, respectively.

Between 1998 and 2000, he was a System Engineer with Motorola Network Solution Sector. Since 2004, he has been with the School of Electrical and Computer Engineering, RMIT University, where he is currently a Research Fellow. His current research interests include microwave photonics devices and subsystems for phased array antenna applications.

Arnan Mitchell (S'97–M'00) received the B.Tech. degree (with honors) in optoelectronics from Macquarie University, Australia, in 1993 and the Ph.D. degree from RMIT University, Melbourne, Australia.

He is a key Researcher with the Microelectronics and Materials Technology Centre, RMIT University, investigating broad-band and specialized integrated optical modulators and radio-frequency (RF) photonic components for communications and signal-processing applications. Currently, he is a Senior Lecturer in the School of Electrical and Computer Engineering, RMIT University. He maintains an active interest in the research of numerical methods required for the design of RF photonic integrated devices and the microtechnologies required to practically realize them.

Kamran Ghorbani received the B.E. degree (with honors) in communication and electronic engineering and the Ph.D. degree from RMIT University, Melbourne, Australia, in 1995 and 2001, respectively.

From 1994 to 1996, he was with the AWA defence industry, where he worked on radar warning receivers. From 1999 to 2001, he was a Senior RF Designer for a telecommunication company. In 2001, he joined the RF Photonic Group, RMIT University, where he is currently a Lecturer. His research interests include integrated optics, phased array antennas, and microwave system design.

Tan-Huat Chio received the B.Eng. degree (with honors) from the National University of Singapore in 1990 and the M.S.E.C.E. and Ph.D. degrees from the University of Massachusetts at Amherst in 1996 and 1999, respectively.

He was a Project Engineer with the Defence Materiel Organization, Singapore, from 1990 to 1994. Since 1999, he has been with DSO National Laboratories, Singapore, where he is currently Head of the Antenna System Laboratories. His current research interest is in wide-band phased array and various beamformers.

Sana Mansoori received the B.Sc. and M.Sc. degrees in electrical engineering from the University of Bahrain in 1992 and 1997, respectively, and the Ph.D. degree from RMIT University, Melbourne, Australia, in 2005.

She joined the University of Bahrain in 1992 as a Graduate Assistant. She was with the Integrated Optics Group, RMIT University. Her research was mainly on photonically implemented microwave filters. Currently, she is an Assistant Professor at the University of Bahrain. Her main areas of interest are signal processing, optical delay line, and photonic transversal filters.

Elias R. Lopez (S'00) received the B.E. degree (with honors) in communication engineering from RMIT University, Melbourne, Australia, in 2004 and the B.E. degree (with honors) in electronic engineering from the Monterrey Institute of Technology for Higher Studies (ITESM), Queretaro, Mexico, in 2004. He is currently pursuing the Ph.D. degree in communication engineering from RMIT University.

His research interest is investigation of hybrid integrated systems.